Optimal Huygens' Metasurface for Wireless Power Transfer Efficiency Improvement

IEEE Access
Multidisciplinary | Rapid Review | Open Access Journal

Received November 9, 2020, accepted November 14, 2020, date of publication November 30, 2020,
date of current version December 11, 2020.

Digital Object Identifier 10.1109/ACCESS.2020.3041337

Optimal Huygens' Metasurface for Wireless Power Transfer Efficiency Improvement

HEMN YOUNESIRAAD[1], MOHAMMAD BEMANI[1], AND LADISLAU MATEKOVITS[2,3,4], (Senior Member, IEEE)

[1]Department of Electrical and Computer Engineering, University of Tabriz, Tabriz 5166616471, Iran
[2]Faculty of Electronics and Telecommunications, Politehnica University Timisoara, 300223 Timisoara, Romania
[3]Istituto di Elettronica e di Ingegneria dell'Informazione e delle Telecomunicazioni, National Research Council, 10129 Turin, Italy
[4]Dipartimento di Elettronicae Telecomunicazioni, Politecnico di Torino, 10129 Torino, Italy

Corresponding author: Ladislau Matekovits (e-mail: ladislau.matekovits@polito.it)

ABSTRACT In this paper, we investigate the electromagnetic response of a Huygens' metasurface (HMS) embedded between the transmitter and receiver coils of a near field wireless power transfer (WPT) system and their interactions for the feasibility of increasing efficiency. To analyze the proposed configuration, we use the point-dipole approximation to describe the electromagnetic fields and boundary conditions governing HMS to calculate the mutual inductance between the coils and to obtain closed-form analytical expressions. The proposed theory shows that by optimally designing the HMS inclusions, the amplitude of the mutual inductance between the transmitter and receiver coils in the near-field WPT can be increased, resulting in improved efficiency. Finally, by drawing on the proposed theory, we design a thin layer and finite-size HMS consisting of 64 elements. The bianisotropic Omega-type particle is used to design the HMS to improve the efficiency of the sample WPT system at the frequency of 100 MHz. The results of the full-wave simulation show that the power transfer efficiency in the free space increases from 25% to 42% in the presence of the proposed HMS.

INDEX TERMS Wireless power transfer, Huygens metasurfaces, power transfer efficiency.

I. INTRODUCTION

By expanding electrical appliances and increasing their fundamental role in everyday human life, the energy supply of these devices is one of the most critical challenges. In the industry, a large number of electronic detectors and compact sensors are often installed in places where access to them is difficult. Also, recent advances in medical sciences have led to the emergence of a wide range of implanted devices (i.e., pacemaker). One of the most innovative and attractive ideas to prevent the ongoing change of electronic batteries and the continuous supply of energy is the concept of wireless power transfer (WPT). WPT is not a new concept and has a potential historical background. Nikola Tesla made the first test of wireless power transmission in the early 20th century [1]. WPT is done in two ways. The first is the power transfer using radiation waves, which is referred to as the far-field WPT while the other is based on the transmission of power through the near-field, which make use of the coupling of the evanescent waves [2]. The near-field-based WPT is divided into two groups of near-magnetic field coupling and near-electric field coupling that are called inductive power transfer (IPT) [3], and capacitive power transfer (CPT) [4], respectively. One of the preferred methods for IPT is magnetic resonance power transfer (MRPT), in which energy can be transmitted between two magnetic resonance devices with the same resonant frequency.

In 2007, an MIT research group proposed the first MRPT system scheme, which transferred 60 watts at a distance of 2 meters with 45% efficiency [5]. There are two essential factors that define the function of MRPT systems: resonator quality factor and coupling factor (or mutual inductance) between the resonators. The modern MRPT systems support power transmissions at moderate distances (2 to 5 times of the resonator's dimensions) [2]. Resonators play a vital role in WPT systems. WPT resonators should be designed and constructed with high Q-factor to prevent unnecessary losses and achieve effective power transmission. Today, a variety of resonators are proposed to improve WPT performance [6]–[13]. For MRPT systems, the power between the resonators is transmitted through the coupling of the evanescent fields. Therefore, the possibility of amplifying the evanescent waves by the metamaterial can be used in this case. In fact, the efficiency of the WPT system can be increased by amplifying the evanescent waves, which can be achieved by placing a

The associate editor coordinating the review of this manuscript and approving it for publication was Shah Nawaz Burokur.

metamaterial with a negative index between the transmitter and the receiver.

Metamaterial has many applications in the field of electromagnetic wave manipulation such as its capabilities in the evanescent waves amplification [14]. Wang performed a WPT experiment using μ-negative (MNG) materials for the first time [15]. Since most WPT systems are based on the near magnetic field coupling, it is sufficient to use an MNG type metamaterial. Recently, a variety of meta media and metamaterial super-lenses have been investigated theoretically [16]–[19] and experimentally [20]–[32] to improve WPT efficiency in the near-field range. Metasurface can be defined as a two-dimensional counterpart of metamaterial state that exhibits attractive electromagnetic responses that are not found in natural materials. It has various applications in various fields, such as perfect electromagnetic absorption [33], conformal transformation optics [34], metasurface antennas [35], nonlinear diatomic metasurface [36], reflection-less zero refractive index [37], creating electromagnetic illusions [38], and mantle cloaking [39]. Recently, much research has been done on increasing the WPT efficiency utilizing metasurface. Smith *et al.* have proposed an ideal holographic metasurface manipulating microwave beam to increase total WPT efficiency [40]. In [41], a metasurface-based smart table was introduced that portable devices wirelessly charged by transforming the evanescent fields into propagating waves which significantly improves the near field coupling. In our recent paper [42], we have investigated the possibility of improving efficiency in non-radiative WPT using a metasurface embedded between two varying current coils based on a point-dipole approximation to achieve a closed-form expression for mutual impedance.

The present paper is divided into two main sections. In the first part, the effect of the presence of the HMS on the near-field WPT performance is theoretically investigated. To analyze the possibility of increasing the efficiency of WPT utilizing the HMS, a magnetic dipole approximation is used such that the transmitter and receiver resonators in the near-field WPT and HMS can be modeled as two magnetic dipoles carrying constant current and fictitious electric and magnetic surface currents, respectively. Then, using electromagnetic wave theory and HMS analytical models, the proposed modeled WPT can be analyzed and the closed-form expressions for mutual inductance between magnetic dipoles and power transfer efficiency can be obtained. In the second part, we investigate a practical WPT system. To improve the efficiency of this system, a suitable HMS is proposed that contains cells that make up a bianisotropic Omega-type particle. This cell can act as an HMS because its structure is such that it can simultaneously generate electrical and magnetic dipole moments.

II. HUYGENS' METASURFACE FOR NEAR-FIELD WPT

In near-field WPT, the power transmission efficiency is dependent on the mutual inductance between the transmitter and receiver coils. Therefore, knowledge of the value of the mutual inductance will be very useful for efficiency calculation. In this section, to analyze the effect of HMS on the performance of the WPT system using the point-dipole approximation, the electromagnetic fields in the presence of HMS can be calculated to obtain an analytical and closed-form expression for mutual induction between coils. Figure 1 illustrates the structure of the WPT in which the transmitter and receiver coils are modeled as magnetic dipoles, with a HMS embedded between them. Let assume that the size of the coils is very small compared to the wavelength so that they can be modeled as magnetic dipoles with current i and area $A_{1,2} = \pi r_{1,2}^2$ as $\overline{m}_{1,2} = iA_{1,2}\hat{n}$ where $\hat{n}$ is a unit vector normal to the plane of the dipoles.

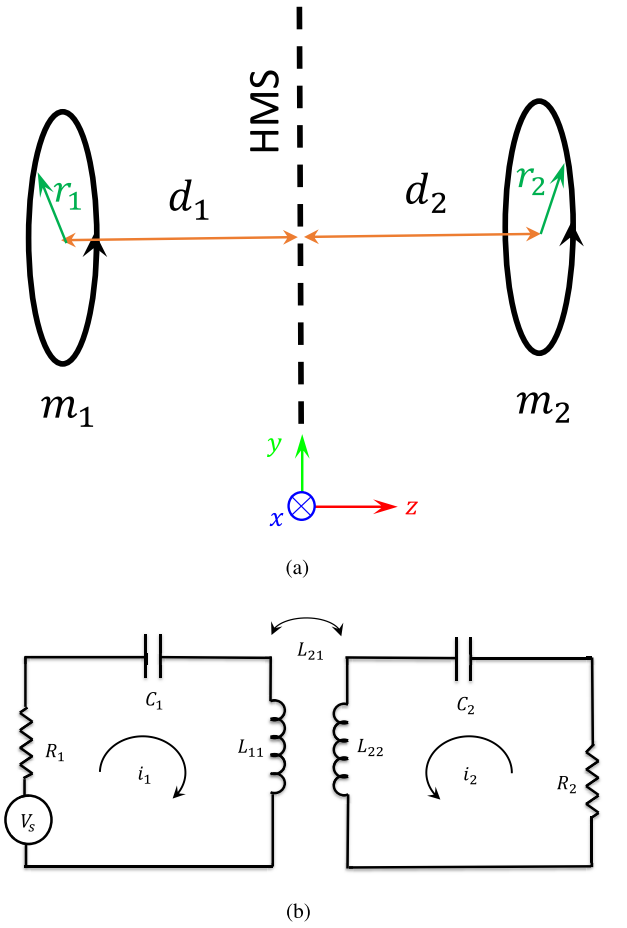

FIGURE 1. (a) The schematic of the proposed implementation sub-wavelength WPT including two single-tern coils (modeled as magnetic dipole moments oriented in the z-direction) and a HMS embedded between them at $z = 0$. The distance from the center of the transmitter coil and receiver coil is d_1 and d_2, respectively. (b) Equivalent circuit diagram of the system.

To calculate the mutual inductance between the dipoles shown in Fig. 1, the mutual inductance is obtained by induced the magnetic field of the transmitter coil at the center of the receiver coil. To do this, we follow the approach given in [43]. The electromagnetic fields of the magnetic dipole can be

calculated as

$$H_{z,1} = -\frac{jm_1}{8\pi}\int_{-\infty}^{+\infty} dk_\rho \frac{k_\rho^3}{k_z} H_0^{(1)}(k_\rho\rho)(e^{jk_z z} + Re^{-jk_z z})e^{jk_z d_1} \tag{1}$$

for $-d_1 < z < 0$ and

$$H_{z,2} = -\frac{jm_1}{8\pi}\int_{-\infty}^{+\infty} dk_\rho \frac{k_\rho^3}{k_z} H_0^{(1)}(k_\rho\rho)(Te^{jk_z z})e^{jk_z d_1} \tag{2}$$

in the region with $z > 0$, where $k_z = \sqrt{(k^2 - k_\rho^2)}$ as well as $k = 2\pi/\lambda$, $H_0^{(1)}(\cdot)$, R and T are wave number, Hankel function of the first kind, zeroth order, reflection and transmission coefficients, respectively. Since the unit vector normal to the plane of the magnetic dipole is in the direction of $\hat{z}$, then this configuration only generates TE fields as described in (1) and (2). To investigate the effect of HMS on the performance of the WPT system and find the mutual inductance between the dipoles, we use the boundary conditions governing the metasurface. In the surface equivalence principle, the electromagnetic fields can be described in reflection and transmission regions. Since the fields are generally discontinuous at $z = 0$, the boundary condition at this plane can be written as [44]

$$j\omega\overline{\overline{\alpha}}_{ee}^{\text{eff}} \cdot E_{t,ave} = \hat{z} \times (\overline{H}_2 - \overline{H}_1) \tag{3a}$$

$$j\omega\overline{\overline{\alpha}}_{mm}^{\text{eff}} \cdot H_{t,ave} = -\hat{z} \times (\overline{E}_2 - \overline{E}_1) \tag{3b}$$

where $\overline{\overline{\alpha}}_{ee}^{\text{eff}}$ and $\overline{\overline{\alpha}}_{mm}^{\text{eff}}$ are dyadic effective electric and magnetic polarizabilities, respectively. Each constituent polarizable particle of the HMS and the coupling between them can be characterized by its electric and magnetic effective polarizabilities. The effective polarizabilities can be introduced by electric sheet admittance ($j\omega\overline{\overline{\alpha}}_{ee}^{\text{eff}} = \overline{\overline{Y}}_{es}$) and magnetic sheet impedance ($j\omega\overline{\overline{\alpha}}_{mm}^{\text{eff}} = \overline{\overline{Z}}_{ms}$). We use the spectral components of the electromagnetic field as below to facilitate the calculation and obtain the desired relationships.

$$\overline{H} = \int_{-\infty}^{+\infty} dk_\rho \widetilde{H}(k_\rho, z, \varphi) \tag{4a}$$

$$\overline{E} = \int_{-\infty}^{+\infty} dk_\rho \widetilde{E}(k_\rho, z, \varphi) \tag{4b}$$

By specifying the spectral component of z, the other components of the electromagnetic field can be determined as

$$\widetilde{E}_y = \frac{j\omega\mu}{k_\rho^2}\frac{\partial \widetilde{H}_z}{\partial x} \tag{5a}$$

$$\widetilde{H}_x = \frac{1}{k_\rho^2}\frac{\partial^2 \widetilde{H}_z}{\partial x \partial z} \tag{5b}$$

In the following, by determining the spectral components of the electromagnetic fields in the reflection and transmission regions and substituting them in the boundary conditions, the reflection and transmission coefficients can be obtained in the whole space as

$$R = \frac{1}{2}\left(\frac{1 - \frac{\omega\mu Y_{es}}{2k_z}}{1 + \frac{\omega\mu Y_{es}}{2k_z}} - \frac{1 - \frac{k_z Z_{ms}}{2\omega\mu}}{1 + \frac{k_z Z_{ms}}{2\omega\mu}}\right) \tag{6a}$$

$$T = \frac{1}{2}\left(\frac{1 - \frac{\omega\mu Y_{es}}{2k_z}}{1 + \frac{\omega\mu Y_{es}}{2k_z}} + \frac{1 - \frac{k_z Z_{ms}}{2\omega\mu}}{1 + \frac{k_z Z_{ms}}{2\omega\mu}}\right) \tag{6b}$$

On the other hand, the electric sheet admittance and magnetic sheet impedance can be written in terms of reflection and transmission coefficients as follows

$$\frac{\omega\mu Y_{es}}{2k_z} = \frac{1 - T - R}{1 + T + R} \tag{7a}$$

$$\frac{k_z Z_{ms}}{2\omega\mu} = \frac{1 - T + R}{1 + T - R} \tag{7b}$$

To obtain the mutual inductance between the magnetic dipoles, we should calculate the magnetic field intensity in the position of the receiver coil. Let assume that the distance between dipoles is deeply sub-wavelength so in the near field region only Fourier components with $|k_\rho| \gg k$ are considered, then the calculations can be significantly simplified. Under this condition, the approximation $-jk_z \cong |k_\rho|$ can be made [35]. By substituting (6b) in (2), the magnetic field can be found in the position of the receiver magnetic dipole as eq. (8), as shown at the bottom of the next page. After calculation of the integral in (8), the flux through the receiver dipole can be obtained as (9), where $E_1(x)$ is the exponential integral and is described as

$$E_1(x) = \int_x^\infty \frac{e^{-t}}{t} dt \tag{10}$$

By dividing eq. (9), as shown at the bottom of the next page, by the current i, the mutual inductance L_{21} can be written as (11), as shown at the bottom of the next page, where $d = d_1 + d_2$ is the distance between the magnetic dipoles. In the next step, we will investigate the interaction of HMS on the self-inductance of the magnetic dipole as mentioned in [16]. The effective magnetic polarizability of the magnetic dipole in the presence of HMS can be written as

$$\alpha_{m,dipole}^{\text{eff}} = (\alpha_{m,dipole}^{-1} - G_{zz}^{\text{ref}})^{-1} \tag{12}$$

where $\alpha_{m,dipole}$ is the intrinsic magnetic polarizability of the magnetic dipole and G_{zz}^{ref} is the reflected portion of the Green's function as follows

$$G_{zz}^{\text{ref}} = \frac{1}{4\pi}\int_0^\infty \frac{1}{2}\left(\frac{1 - \frac{\omega\mu Y_{es}}{2k_z}}{1 + \frac{\omega\mu Y_{es}}{2k_z}} - \frac{1 - \frac{k_z Z_{ms}}{2\omega\mu}}{1 + \frac{k_z Z_{ms}}{2\omega\mu}}\right) e^{-2k_\rho d_1} k_\rho^2 dk_\rho \tag{13}$$

Under this condition and using $\varphi_1 = L_{11} i$ as well as $L_{11} = \mu A_1^2/\alpha_{m,dipole}$, the self-inductance of the dipole can be found as

$$L_{11} = L_{11}^{(0)} - \mu A_1^2 G_{zz}^{\text{ref}} = L_{11}^{(0)} + L_{11}^{(1)} \tag{14}$$

where $L_{11}^{(1)}$ is defined as the HMS contribution to self-inductance of the transmitter coil and $L_{11}^{(0)}$ is the self-inductance of the dipole without HMS.

A. CALCULATION OF EFFICIENCY

In this section, we calculate the WPT efficiency of the configuration illustrated in Fig. 1. Fig. 1(b) shows the circuit model of the structure, in which we assume that the transmitter and receiver coils are connected to an external circuit with resistor R and capacitor C and the transmitter coil is excited by a voltage source. The expression presented in [16] is defined as the ratio of the delivered power to the resistive load R_2 to the total consumed power, as the power transfer efficiency.

$$\eta = \frac{R_2}{R_2^{\text{eff}}}\frac{\chi}{1+\chi} \tag{15}$$

where

$$\chi = \frac{R_2^{\text{eff}}\omega^2|L_{21}|^2}{R_1^{\text{eff}}|R_2 + j\omega L_{22} + 1/j\omega C_2|^2} \tag{16}$$

where

$$R_1^{\text{eff}} = R_1 - \omega\text{Im}(L_{11}) + \omega^2\text{Im}\Big(\frac{L_{12}L_{21}}{R_2 + j\omega L_{22} + 1/j\omega C_2}\Big) \tag{17}$$

$$R_2^{\text{eff}} = R_2 - \omega\text{Im}(L_{22}) + \omega^2\text{Im}\Big(\frac{L_{12}L_{21}}{R_1 + j\omega L_{11} + 1/j\omega C_1}\Big) \tag{18}$$

The efficiency expression confirms that by maximizing the parameter χ, we can achieve efficiency close to 100%. Also, to maximize efficiency, the ratio R_2^{eff}/R_2 should be as small as possible. As mentioned earlier, the maximum WPT efficiency of MRPT occurs at the resonant frequency corresponding to the coils. The resonant frequency of the coils can be adjusted by varying the capacitance value. In (17) and (18), one can help maximize efficiency by removing the imaginary part of the self-inductance. Normally the self-inductance of the coils is a real value, but the electromagnetic interaction between magnetic dipoles and HMS can affect the self-inductance of the coils and add an imaginary part. The last term in (17) and (18) can be neglected concerning the L_{21} and ω. To maximize efficiency, the mutual inductance L_{21} must be as large as possible. To analyze the efficiency relationship, we define the following parameter as the ratio of mutual inductance in the presence of the HMS to the mutual inductance in free space.

$$\rho = \frac{L_{21}}{L_{21}^{vac}} \tag{19}$$

where

$$L_{21}^{vac} = -\frac{\mu A_1 A_2}{2\pi d^3} \tag{20}$$

As mentioned in [16]–[32], the idea of using metamaterial in WPT comes from its ability to amplify evanescent fields and wavefront manipulation of electromagnetic waves. In fact, the metamaterial acts as a super-lens and refocuses the magnetic field generated by the transmitter coil to the center of the receiver coil as far as possible. Therefore, our goal in this section is to obtain optimal constituent particles of HMS so that the evanescent fields can be amplified as much as possible and the parameter ρ can be maximized, and the mutual inductance and thus the maximum efficiency can be achieved. It can be shown that equation (11) is maximized when $(\omega\mu Y_{es})/2j = -2\omega\mu/jZ_{ms}$ or $Y_{es}Z_{ms} = -4$. This result is consistent with the proven expression in [45]. Like that shown in [45] at a surface mode resonance $R \to \infty$ so, under this condition, the reflection coefficient can be minimized whereas the transmission coefficient can be as close to the unit as possible. Since $E_1(x)$ has an imaginary part for negative values of x, so assuming $Y_{es}Z_{ms} = -4$ in addition to maximizing mutual inductance, the self-inductance of the coils has no imaginary part, which leads to increase the efficiency. According to the discussions as mentioned above, the mutual inductance in the presence of the HMS is as follows

$$L_{21} = \frac{\mu A_1 A_2}{4\pi}\Bigg(\frac{qk}{d^2} + \Big(\frac{qk}{2}\Big)^3\Big(e^{qkd/2}E_1(qkd/2) + e^{-qkd/2}E_1(-qkd/2)\Big)\Bigg) \tag{21}$$

$$H_{z,2} = -\frac{m_1}{8\pi}\int_0^{+\infty} dk_\rho k_\rho^2 H_0^{(1)}(k_\rho\rho)\Big(\frac{k_\rho - \frac{\omega\mu Y_{es}}{2j}}{k_\rho + \frac{\omega\mu Y_{es}}{2j}} - \frac{k_\rho - \frac{2\omega\mu}{jZ_{ms}}}{k_\rho + \frac{2\omega\mu}{jZ_{ms}}}\Big)e^{-k_\rho(d_1+z)} \tag{8}$$

$$\varphi_2(\rho=0, z=d_2) = \int B_{z,2}.ds = \frac{\mu A_1 A_2 i}{4\pi}\Bigg(\Big(\frac{(\frac{\omega\mu Y_{es}}{2j})^2}{-d} + \frac{(\frac{\omega\mu Y_{es}}{2j})}{(-d)^2} + \frac{1}{(-d)^3} + (\frac{\omega\mu Y_{es}}{2j})^3 e^{\frac{\omega\mu Y_{es}d}{2j}}E_1\Big(\frac{\omega\mu Y_{es}d}{2j}\Big)\Big) - \Big(\frac{(\frac{2\omega\mu}{j54Z_{ms}})^2}{-d} + \frac{(\frac{2\omega\mu}{jZ_{ms}})}{(-d)^2} + \frac{1}{(-d)^3} + (\frac{2\omega\mu}{jZ_{ms}})^3 e^{\frac{2\omega\mu d}{jZ_{ms}}}E_1\Big(\frac{2\omega\mu d}{jZ_{ms}}\Big)\Big)\Bigg) \tag{9}$$

$$L_{21} = \frac{\mu A_1 A_2}{4\pi}\Bigg(\Big(\frac{(\frac{\omega\mu Y_{es}}{2j})^2}{-d} + \frac{(\frac{\omega\mu Y_{es}}{2j})}{(-d)^2} + \frac{1}{(-d)^3} + (\frac{\omega\mu Y_{es}}{2j})^3 e^{\frac{\omega\mu Y_{es}d}{2j}}E_1\Big(\frac{\omega\mu Y_{es}d}{2j}\Big)\Big) - \Big(\frac{(\frac{2\omega\mu}{jZ_{ms}})^2}{-d} + \frac{(\frac{2\omega\mu}{jZ_{ms}})}{(-d)^2} + \frac{1}{(-d)^3} + (\frac{2\omega\mu}{jZ_{ms}})^3 e^{\frac{2\omega\mu d}{jZ_{ms}}}E_1\Big(\frac{2\omega\mu d}{jZ_{ms}}\Big)\Big)\Bigg) \tag{11}$$

Also, HMS contribution to self-inductance L_{11} can be calculated as

$$L_{11}^{(1)} = -\frac{\mu A_1^2}{4\pi}\left(\frac{qk}{d_1} + \frac{1}{d_1^3}\right) \tag{22}$$

The expression for $L_{22}^{(2)}$ is obtained by replacing d_1 and A_1 with d_2 and A_2, respectively. In the above equations, the electric sheet admittance is considered as $Y_{es} = -q/j\eta_0$ wherein η_0 is the intrinsic impedance in free space. The parameter q is an arbitrary variable to normalize the electric sheet admittance and varying from 0 to 150 to obtain Fig. 2. We investigate the point-dipole approximation based WPT at a maximum distance of $0.1\lambda_0$ between the magnetic dipoles to guarantee the sub-wavelength WPT conditions where λ_0 is the wavelength corresponding to the resonant frequency. For and example, consider a near-field WPT system at the interesting frequency of 100 MHz. The variation of the parameter ρ as a function of the distance between the coils and different values of q is shown in Fig. 2 obtained using (19), (20), and (21). It can be seen from the figure, the value of this parameter is maximum for $q = 10$ at $0.1\lambda_0$ (the maximum possible distance that can guarantee the sub-wavelength WPT condition). This figure shows that the use of HMS, especially at longer distances of sub-wavelength WPT, can greatly improve mutual inductance. Since mutual inductance in the absence of HMS is reduced with a ratio of $\sim 1/d^3$, therefore, according to L_{21} expression, utilizing HMS can be a suitable solution for improvement of efficiency of near-field WPT.

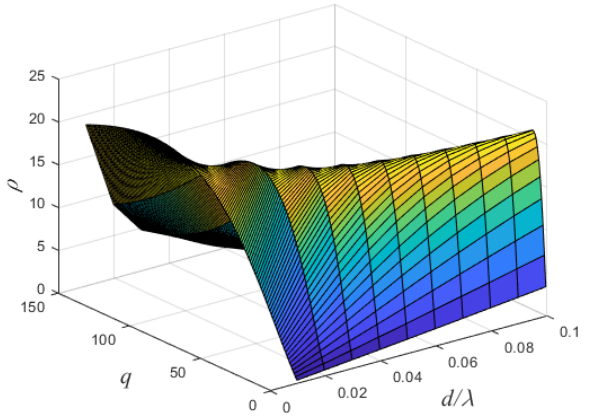

FIGURE 2. The 3D diagram of a variation of the parameter ρ as a function of the distance between the coils and different values of q at 100 MHz.

Using Eqs. (15), (16), (17), (18), and (21), efficiency can be obtained in terms of frequency. Figure 3 shows the efficiency of WPT without metasurface and WPT in the presence of HMS embedded between the coils for different frequencies at a distance of $0.1\lambda_0$. To obtain the efficiency when a metasurface is embedded between the coils, the expression for mutual

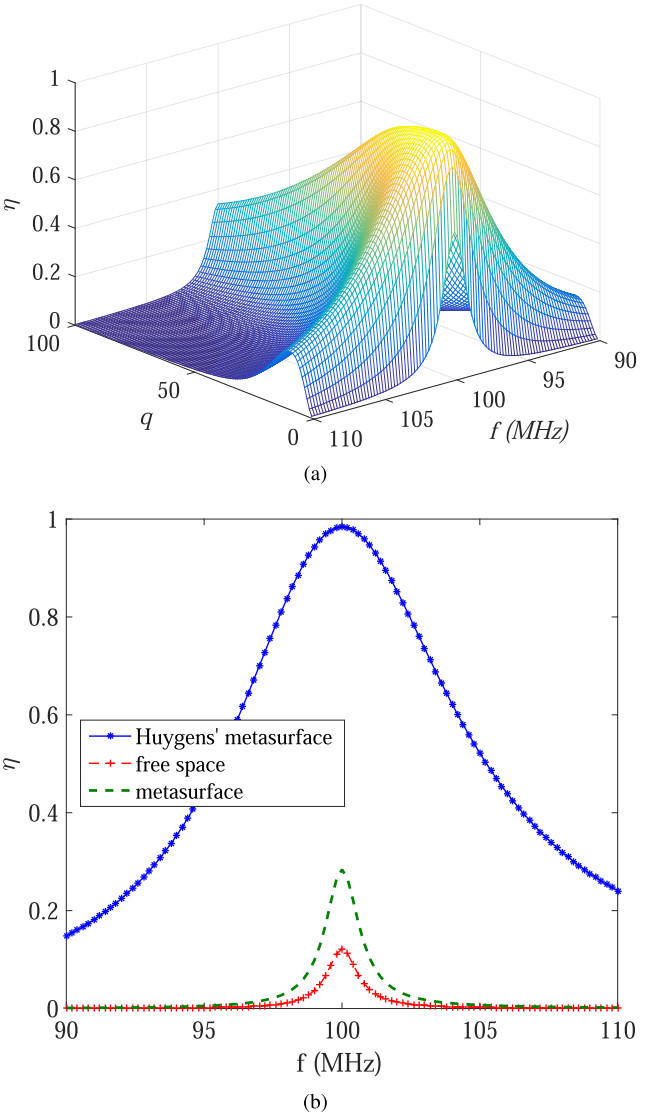

FIGURE 3. (a) The 3D diagram of a variation of efficiency as a function of frequency and different values of q (b) Comparison of efficiency as a function of frequency between proposed HMS-assisted WPT and metasurface-assisted WPT as well as conventional WPT.

inductance in [42] is used, which is as follows.

$$L_{21}^{\mathrm{MS}} = \frac{-j\mu_0 A_1 A_2}{32\pi Z_s^3}\left(\left(\frac{2jZ_s\omega^2\mu_0^2}{d} + \frac{4Z_s^2\omega\mu_0}{d^2} - \frac{16jZ_s^3}{d^3}\right) - (\omega\mu_0)^3 e^{\frac{d\omega\mu_0}{2jZ_s}} E_1\left(\frac{d\omega\mu_0}{2jZ_s}\right)\right) \tag{23}$$

where Z_s is the equivalent surface impedance of the metasurface. As shown in Fig. 3(a) the maximum efficiency occurs at the resonant frequency corresponding to the coils, as expected. At the same frequency, it can be seen that use of HMS can greatly increase efficiency within a distance of $0.1\lambda_0$ between coils so that efficiency reaches from 10% to 95% for the conventional WPT compared to HMS-assisted WPT. As shown in Fig. 3, at the resonance frequency, choosing $q = 10$ yields the highest possible

efficiency. In this case, in addition to achieving maximum efficiency, the widest possible bandwidth is also observed. In fact, HMS with $Y_{es} = -10/j\eta_0$ can determine the optimal effective polarizabilities, α_{ee}^{eff} and α_{mm}^{eff}, that form the desired HMS. By wise choice of the optimal effective polarizability, we can expect the evanescent fields to be significantly amplified, and this will increase the efficiency as well as it will give rise to bandwidth enhancement of WPT. Comparison of efficiency as a function of frequency between proposed Huygens' metasurface-assisted WPT and presented implementation in [42] as well as conventional WPT is shown in Fig. 3(b). It can be seen from the figure, that the proposed implementation report better performance compared to the previous work presented in [42] and the conventional system, proving that utilizing HMS with optimal electric and magnetic effective polarizability can not only increase efficiency by amplifying evanescent fields and increasing coupling between coils, but also can yield bandwidth enhancement.

Figure 4(a) shows the efficiency variation as a function of the distance between the coils and different values of q at the resonant frequency. It can be seen from the figure that at a distance of $0.1\lambda_0$ the maximum efficiency is obtained for $q = 10$. As the figure shows, for WPT in the absence of HMS, the efficiency drops with a ratio of $\sim 1/d^6$ whereas utilizing HMS between the coils causes a little change in efficiency as the distance between the coils increases, and the proposed implementation can be expected to have a much lower efficiency drop compared to the conventional WPT. In fact, with increasing distance, the perception of the impact of HMS on the efficiency of the power transmission and the coupling between the coils as well as the amplification of the evanescent fields are more noticeable. In other words, in this case, the HMS assembled between the coils can recapture the near-field magnetic field and amplifies it by increasing efficiency and refocusing it on the receiver coil. Carefully considering the calculated mutual impedance expression including the effect of the HMS in this section and omitting the term of $1/d^3$ in the expression, one can expect the efficiency to drop much lower compared to the conventional WPT by choosing the optimal effective electric and magnetic polarizability with increasing distance between the coils. Figure 4(b) illustrates the comparison of efficiency as a function of the distance between the coils between proposed HMS-assisted WPT and presented implementation in [42] as well as conventional WPT.

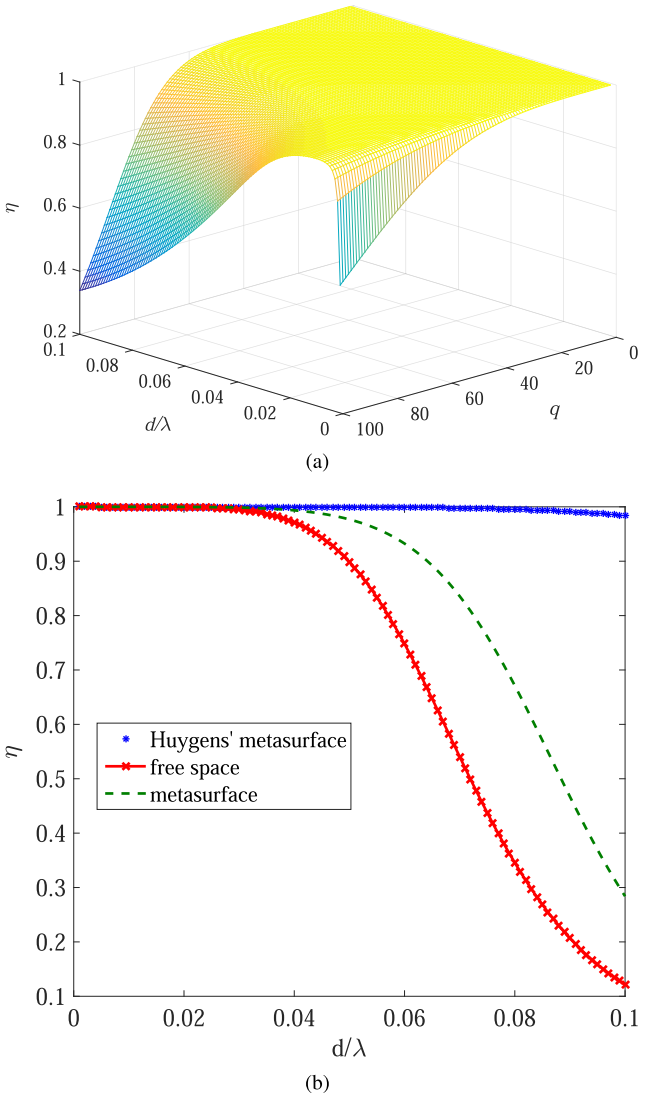

FIGURE 4. (a) The 3D diagram of a variation of efficiency as a function of the distance between the coils and different values of q. (b) Comparison of efficiency as a function of the distance between the coils between proposed HMS-assisted WPT and metasurface-assisted WPT as well as conventional WPT.

III. A REALIZABLE HMS DESIGN FOR WPT EFFICIENCY IMPROVEMENT

In this section, we apply the theory presented in Section II to design a metasurface-assisted WPT at 100 MHz. Figure 5 shows the configuration of the studied WPT in which the two resonators, as transmitter and receiver loops, are 40 cm apart and position a thin finite-size HMS layer in the middle of them. Figure 5(b) shows the geometry of the resonator of the WPT system. To realize the impedance matching and adjust the resonance frequency of the WPT system, the two capacitors are considered as the impedance matching circuit to match with 50Ω. For the resonator, using the full-wave simulation by HFSS software the optimum radius $r = 16$ cm with a wire thickness of $w = 1.5$ cm, as well as $C_p = 0.95$ pF and $C_s = 0.8$ pF is obtained. The proposed cell shown in Fig. 5(c) is used to design and implement the thin, finite-size and realizable desired HMS for increasing WPT efficiency. In this particle, the induced moment and the field vector are orthogonal. In this case, HMS can be implemented by combining a loop and a straight electric dipole antenna to have a simultaneous electrical and magnetic response, as illustrated in Fig. 5(c). This planar geometry often referred to as the omega meta-atom [46]–[48], enables magnetoelectric polarization orthogonal to the exciting field. One of these special inclusions is a split-ring resonator as the omega inclusion depicted in Fig. 5(c).

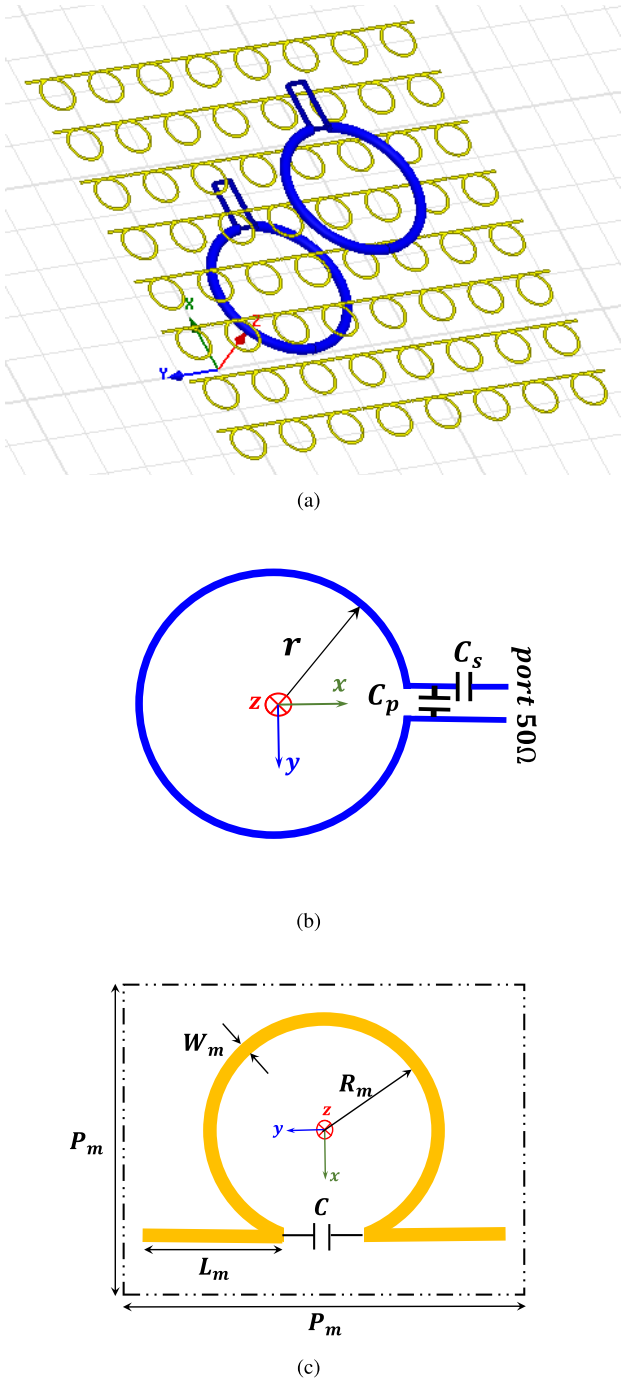

FIGURE 5. (a) Configuration of the proposed HMS-assisted WPT system including two resonators and an HMS positioned between them, (b) sketch of the transmitter(receiver) resonator, and (c) sketch of the Omega-type particle forming the desired HMS.

The overall HMS consists of an 8 × 8 array of this proposed cell. The dimensions of the proposed sub-wavelength inclusion can be determined using calculated optimal effective quasistatic electric and magnetic polarizabilities and the approaches presented in [49] and [50] to determine the full polarizability tensor of sub-wavelength particles with arbitrary shape and composition. The optimized parameters are $R_m = 40.92$ mm, $W_m = 5.47$ mm, $L_m = 53.78$ mm, $P_m = 126.5$ mm and $C = 21$ pF.

As this cell is used for many different applications in microwave frequencies and can be implemented with both plasmonic [51], [52] and dielectric [53], [54] materials, we place a capacitor between the two horizontal arms (straight electric dipole antenna) to allow for the design and implementation of the desired HMS with limited dimensions. The value of this capacitor and the inductor due to the conductor parts of the inclusion can adjust the resonance frequency of the WPT system. The geometrical dimension of the proposed cell and the corresponding capacitance value is optimized by HFSS software. It should be noted that in the extraction of the effective quasistatic electric and magnetic polarizabilities values of constituent particles formed the HMS obtained in section II, the magnetoelectric polarizability dyadics of the proposed cells is neglected. An Omega inclusion can have non-zero magnetoelectric polarizability and act as a bi-anisotropic inclusion when the induced moment (e.g., $\overline{m}$) and the field vector ($\overline{E}_{\rm loc}$) are orthogonal. Therefore it provides magnetoelectric polarization orthogonal to the exciting field. The index "loc" indicates that if the meta-atom is positioned in an array, these fields are the local fields which excite this particular meta-atom. In contrast the mentioned configuration, in our proposed HMS, the direction of the electric field vector is parallel to the induced moment. Besides, the Omega has a mirror symmetry in both directions of the wave propagation along the $\pm z$. In other words, the electromagnetic response is the same for both propagation directions in both amplitude and phase, so with this configuration, the magnetoelectric coefficient can be neglected [55]. To validate the theory presented in this work with full-wave simulations, the proposed cell has been simulated to obtain the corresponding equivalent surface electric admittance and surface magnetic impedance. Figure 6 shows the parameter of $Y_{es}Z_{ms}$ as a function of frequency. As shown in the figure, the proposed cell has a resonant frequency at the

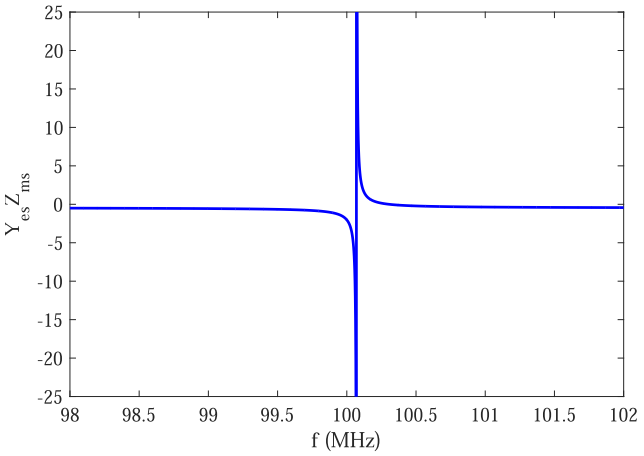

FIGURE 6. Simulated parameter of $Y_{es}Z_{ms}$ as a function of frequency for the proposed cell.

frequency of 100 MHz. According to the theory presented in the previous section, when $Y_{es}Z_{ms} = -4$, HMS can amplify the evanescent near-field and the amplitude of mutual inductance between the resonators, and consequently, it will increase power transmission efficiency. As shown in Fig. 6 the condition $Y_{es}Z_{ms} = -4$ is established around the design frequency. The simulated parameter of $q = 6.5$ is obtained for the optimized proposed cell.

Figure 7 depicts the WPT efficiency as a function of frequency for the WPT without HMS and WPT in the presence of the designed HMS. As shown in the figure, the power transfer efficiency is increased from 25% in the conventional mode to 42% in the HMS-assisted WPT. The simulation results in this figure show that the engineered HMS located between the resonators by amplifying the evanescent fields at the resonant frequency can increase the efficiency in the range $0.1\lambda_0$ to about 68%. In the full-wave simulation, WPT efficiency can be estimated by calculating the expression of $|S_{21}|^2$. In section II, the ultra-thin HMS is considered as an infinite ideal homogeneous and low-dispersive layer, whose electromagnetic response to external fields can be described through equivalent electric sheet admittance and magnetic sheet impedance based on Huygens' principle. Proven expressions for mutual inductance and efficiency for this type of HMS are in the ideal case, leading to maximum efficiency. While in the simulation setup, a two-dimensional array of 8×8 real cells is used to implement the required HMS, which affects efficiency. It is clear that by presenting novel and more efficient cells, a more robust magnetic response can be achieved using the theory of section II to amplify evanescent waves. In other words, it is possible to increase efficiency by using different cells. The main challenge in real HMS implementation is to design suitable cells at MHz frequencies. The presented expressions in [16] provide the same explanation and observations for the metamaterials. In fact, an ideal meta lens leads to 100% efficiency, while the implementation of a perfect lens with the same performance obtained from the theory as mentioned in the literature is impossible and therefore the simulation results with the analytical results of using infinite ideal meta lens with 100% focus is different. One should also mention that the considered HMS is dispersive, that in turn will affect the performances of the real-life geometry with respect to the ideal case.

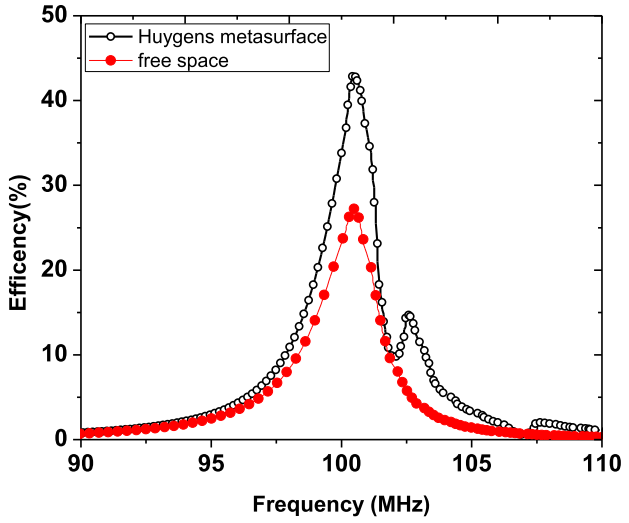

FIGURE 7. Simulated power transfer efficiency for the proposed WPT with and without the HMS at a distance of 40 cm.

Figure 8 shows the magnitude of the magnetic field distribution on a symmetric plane for the proposed WPT. It can be deduced from the figure, by placing the HMS in the middle of two resonators the evanescent field is amplified around it, this increases the coupling between the resonators and thereby increases the WPT efficiency. By comparing Fig. 8(a) and 8(b), it can be concluded that the magnetic flux in the receiver resonator increases in the presence of the HMS, which improves the efficiency.

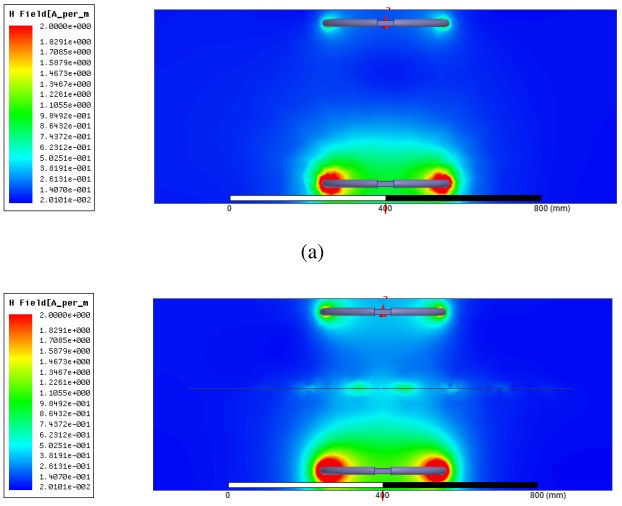

FIGURE 8. Simulated magnetic field distribution between the resonators for (a) WPT without the HMS, and (b) with the HMS at 100 MHz.

IV. CONCLUSION

We have presented a rigorous analysis to describe the electromagnetic fields of the constitutive coils of a HMS-based WPT. First we have calculated the mutual inductance between the coils considering the interaction of them and metasurface using the boundary condition governing the HMS. Then, we have found optimum electric and magnetic polarizabilities as $\alpha_{ee}^{\text{eff}} = 10/\omega\eta_0$, and $\alpha_{mm}^{\text{eff}} = 2\eta_0/5\omega$ that can reach the efficiency from 10% to 95% at the maximum possible distance of a sub-wavelength WPT. The results obtained from the theory show that with the optimal design of HMS, the efficiency and bandwidth can be enhanced simultaneously at the resonant frequency, and the efficiency drops with a very low gradient by increasing the distance between the coils of the sub-wavelength WPT. Then,

using the proposed theory and proven analytical expressions, we designed a WPT system in which we employed an HMS to improve power transfer efficiency. The proposed HMS consists of 64 Omega-type particles that by amplifying the evanescent fields can increase the efficiency of the mentioned WPT system by 68%. The analytical and full-wave simulation results show that by designing novel HMS and utilizing optimization algorithms, the power transfer efficiency can be significantly increased in future works.

REFERENCES

[1] N. Tesla, "Apparatus for transmitting electrical energy," U.S. Patent 1 119 732 A, Dec. 1, 1914.

[2] M. Song, P. Belov, and P. Kapitanova, "Wireless power transfer inspired by the modern trends in electromagnetics," *Appl. Phys. Rev.*, vol. 4, no. 2, Jun. 2017, Art. no. 021102.

[3] C. Zheng, H. Ma, J.-S. Lai, and L. Zhang, "Design considerations to reduce gap variation and misalignment effects for the inductive power transfer system," *IEEE Trans. Power Electron.*, vol. 30, no. 11, pp. 6108–6119, Nov. 2015.

[4] J. Dai and D. C. Ludois, "A survey of wireless power transfer and a critical comparison of inductive and capacitive coupling for small gap applications," *IEEE Trans. Power Electron.*, vol. 30, no. 11, pp. 6017–6029, Nov. 2015.

[5] A. Kurs, A. Karalis, R. Moffatt, J. D. Joannopoulos, P. Fisher, and M. Soljacic, "Wireless power transfer via strongly coupled magnetic resonances," *Science*, vol. 317, no. 5834, pp. 83–86, Jul. 2007.

[6] K. Chen and Z. Zhao, "Analysis of the double-layer printed spiral coil for wireless power transfer," *IEEE J. Emerg. Sel. Topics Power Electron.*, vol. 1, no. 2, pp. 114–121, Jun. 2013.

[7] S. Khan and G. Choi, "Analysis and optimization of four-coil planar magnetically coupled printed spiral resonators," *Sensors*, vol. 16, no. 8, p. 1219, Aug. 2016.

[8] X. Shi, C. Qi, M. Qu, S. Ye, G. Wang, L. Sun, and Z. Yu, "Effects of coil shapes on wireless power transfer via magnetic resonance coupling," *J. Electromagn. Waves Appl.*, vol. 28, no. 11, pp. 1316–1324, Jul. 2014.

[9] M. Song, P. Belov, and P. Kapitanova, "Wireless power transfer based on dielectric resonators with colossal permittivity," *Appl. Phys. Lett.*, vol. 109, no. 22, Nov. 2016, Art. no. 223902.

[10] M. Song, I. Iorsh, P. Kapitanova, E. Nenasheva, and P. Belov, "Wireless power transfer based on magnetic quadrupole coupling in dielectric resonators," *Appl. Phys. Lett.*, vol. 108, no. 2, Jan. 2016, Art. no. 023902.

[11] E. M. Thomas, J. D. Heebl, C. Pfeiffer, and A. Grbic, "A power link study of wireless non-radiative power transfer systems using resonant shielded loops," *IEEE Trans. Circuits Syst. I, Reg. Papers*, vol. 59, no. 9, pp. 2125–2136, Sep. 2012.

[12] B. B. Tierney and A. Grbic, "Planar shielded-loop resonators," *IEEE Trans. Antennas Propag.*, vol. 62, no. 6, pp. 3310–3320, Jun. 2014.

[13] B. B. Tierney and A. Grbic, "Design of self-matched planar loop resonators for wireless nonradiative power transfer," *IEEE Trans. Microw. Theory Techn.*, vol. 62, no. 4, pp. 909–919, Apr. 2014.

[14] T. J. Cui, D. R. Smith, and R. Liu, *Metamaterials: Theory, Design, and Applications*. New York, NY, USA: Springer, 2010.

[15] W. C. Brown and E. E. Eves, "Beamed microwave power transmission and its application to space," *IEEE Trans. Microw. Theory Techn.*, vol. 40, no. 6, pp. 1239–1250, Jun. 1992.

[16] Y. Urzhumov and D. R. Smith, "Metamaterial-enhanced coupling between magnetic dipoles for efficient wireless power transfer," *Phys. Rev. B, Condens. Matter*, vol. 83, no. 20, May 2011, Art. no. 205114.

[17] Y. Zhao and E. Leelarasmee, "Controlling the resonances of indefinite materials for maximizing efficiency in wireless power transfer," *Microw. Opt. Technol. Lett.*, vol. 56, no. 4, pp. 867–875, Apr. 2014.

[18] L. Zhu, X. Luo, and H. Ma, "Distant and wide range wireless power transfer from metamedia," *Appl. Phys. Lett.*, vol. 109, no. 2, Jul. 2016, Art. no. 024103.

[19] L. Zhu, X. Luo, and H. Ma, "Extended explanation of transformation optics for metamaterial-modified wireless power transfer systems," *J. Appl. Phys.*, vol. 119, no. 11, Mar. 2016, Art. no. 115105.

[20] M. J. Chabalko, J. Besnoff, and D. S. Ricketts, "Magnetic field enhancement in wireless power with metamaterials and magnetic resonant couplers," *IEEE Antennas Wireless Propag. Lett.*, vol. 15, pp. 452–455, 2016.

[21] M. J. Chabalko and A. P. Sample, "Electromagnetic time reversal focusing of near field waves in metamaterials," *Appl. Phys. Lett.*, vol. 109, no. 26, Dec. 2016, Art. no. 263901.

[22] B.-J. Che, G.-H. Yang, F.-Y. Meng, K. Zhang, J.-H. Fu, Q. Wu, and L. Sun, "Omnidirectional non-radiative wireless power transfer with rotating magnetic field and efficiency improvement by metamaterial," *Appl. Phys. A, Solids Surf.*, vol. 116, no. 4, pp. 1579–1586, Sep. 2014.

[23] J.-F. Chen, Z. Hu, S. Wang, M. Liu, Y. Cheng, Z. Ding, B. Wei, and S. Wang, "Application of ultra-thin assembled planar metamaterial for wireless power transfer system," *Prog. Electromagn. Res. C*, vol. 65, pp. 153–162, 2016.

[24] Y. Z. Cheng, J. Jin, W. L. Li, J. F. Chen, B. Wang, and R. Z. Gong, "Indefinite-permeability metamaterial lens with finite size for miniaturized wireless power transfer system," *AEU-Int. J. Electron. Commun.*, vol. 70, no. 9, pp. 1282–1287, Sep. 2016.

[25] Y. Fan, L. Li, S. Yu, C. Zhu, and C.-H. Liang, "Experimental study of efficient wireless power transfer system integrating with highly sub-wavelength metamaterials," *Prog. Electromagn. Res.*, vol. 141, pp. 769–784, 2013.

[26] D. Huang, Y. Urzhumov, D. R. Smith, K. H. Teo, and J. Zhang, "Magnetic superlens-enhanced inductive coupling for wireless power transfer," *J. Appl. Phys.*, vol. 111, no. 6, Mar. 2012, Art. no. 064902.

[27] G. Lipworth, J. Ensworth, K. Seetharam, D. Huang, J. S. Lee, P. Schmalenberg, T. Nomura, M. S. Reynolds, D. R. Smith, and Y. Urzhumov, "Magnetic metamaterial superlens for increased range wireless power transfer," *Sci. Rep.*, vol. 4, no. 1, p. 3642, May 2015.

[28] J. Prat-Camps, C. Navau, and A. Sanchez, "Experimental realization of magnetic energy concentration and transmission at a distance by metamaterials," *Appl. Phys. Lett.*, vol. 105, no. 23, Dec. 2014, Art. no. 234101.

[29] A. L. A. K. Ranaweera, T. P. Duong, and J.-W. Lee, "Experimental investigation of compact metamaterial for high efficiency mid-range wireless power transfer applications," *J. Appl. Phys.*, vol. 116, no. 4, Jul. 2014, Art. no. 043914.

[30] E. S. Gamez Rodriguez, A. K. Ramrakhyani, D. Schurig, and G. Lazzi, "Compact low-frequency metamaterial design for wireless power transfer efficiency enhancement," *IEEE Trans. Microw. Theory Techn.*, vol. 64, no. 5, pp. 1644–1654, May 2016.

[31] B. Wang, K. H. Teo, T. Nishino, W. Yerazunis, J. Barnwell, and J. Zhang, "Experiments on wireless power transfer with metamaterials," *Appl. Phys. Lett.*, vol. 98, no. 25, Jun. 2011, Art. no. 254101.

[32] Y. J. Yoo, C. Yi, J. S. Hwang, Y. J. Kim, S. Y. Park, K. W. Kim, J. Y. Rhee, and Y. Lee, "Experimental realization of tunable metamaterial hyper-transmitter," *Sci. Rep.*, vol. 6, no. 1, p. 33416, Dec. 2016.

[33] Y. Ra'di, C. R. Simovski, and S. A. Tretyakov, "Thin perfect absorbers for electromagnetic waves: Theory, design, and realizations," *Phys. Rev. A, Gen. Phys.*, vol. 3, no. 3, Mar. 2015, Art. no. 037001.

[34] G. Ruffato and F. Romanato, "Design of continuously variant metasurfaces for conformal transformation optics," *Opt. Exp.*, vol. 28, no. 23, pp. 34201–34218, 2020.

[35] M. F. Imani, J. N. Gollub, O. Yurduseven, A. V. Diebold, M. Boyarsky, T. Fromenteze, L. Pulido-Mancera, T. Sleasman, and D. R. Smith, "Review of metasurface antennas for computational microwave imaging," *IEEE Trans. Antennas Propag.*, vol. 68, no. 3, pp. 1860–1875, Mar. 2020.

[36] N. Mao, J. Deng, X. Zhang, Y. Tang, M. Jin, Y. Li, X. Liu, K. Li, T. Cao, K. Cheah, H. Wang, J. Ng, and G. Li, "Nonlinear diatomic metasurface for real and Fourier space image encoding," *Nano Lett.*, vol. 20, no. 10, pp. 7463–7468, Oct. 2020.

[37] S. Takehito and H. Asada, "Reflectionless zero refractive index metasurface in the terahertz waveband," *Opt. Exp.*, vol. 28, no. 15, pp. 21509–21521, 2020.

[38] T. J. Smy, S. A. Stewart, and S. Gupta, "Surface susceptibility synthesis of metasurface holograms for creating electromagnetic illusions," *IEEE Access*, vol. 8, pp. 93408–93425, 2020.

[39] H. Younesiraad, M. Bemani, and S. Nikmehr, "Scattering suppression and cloak for electrically large objects using cylindrical metasurface based on monolayer and multilayer mantle cloak approach," *IET Microw., Antennas Propag.*, vol. 13, no. 3, pp. 278–285, Feb. 2019.

[40] D. R. Smith, V. R. Gowda, O. Yurduseven, S. Larouche, G. Lipworth, Y. Urzhumov, and M. S. Reynolds, "An analysis of beamed wireless power transfer in the fresnel zone using a dynamic, metasurface aperture," *J. Appl. Phys.*, vol. 121, no. 1, Jan. 2017, Art. no. 014901.

[41] M. Song, K. Baryshnikova, A. Markvart, P. Belov, E. Nenasheva, C. Simovski, and P. Kapitanova, "Smart table based on a metasurface for wireless power transfer," *Phys. Rev. A, Gen. Phys.*, vol. 11, no. 5, May 2019, Art. no. 054046.
[42] H. Younesiraad and M. Bemani, "Analysis of coupling between magnetic dipoles enhanced by metasurfaces for wireless power transfer efficiency improvement," *Sci. Rep.*, vol. 8, no. 1, p. 14865, Dec. 2018.
[43] W. C. Chew, *Waves and Fields in Inhomogeneous Media*. New York, NY, USA: IEEE press, 1995.
[44] C. Pfeiffer and A. Grbic, "Metamaterial Huygens' surfaces: Tailoring wave fronts with reflectionless sheets," *Phys. Rev. Lett.*, vol. 110, no. 19, May 2013, Art. no. 197401.
[45] S. Maslovski, S. Tretyakov, and P. Alitalo, "Near-field enhancement and imaging in double planar polariton-resonant structures," *J. Appl. Phys.*, vol. 96, no. 3, pp. 1293–1300, Aug. 2004.
[46] S. A. Tretyakov and A. A. Sochava, "Proposed composite material for nonreflecting shields and antenna radomes," *Electron. Lett.*, vol. 29, no. 12, pp. 1048–1049, Jun. 1993.
[47] M. M. I. Saadoun and N. Engheta, "A reciprocal phase shifter using novel pseudochiral or Ω medium," *Microw. Opt. Technol. Lett.*, vol. 5, no. 4, pp. 184–188, Apr. 1992.
[48] C. R. Simovski, S. A. Tretyakov, A. A. Sochava, B. Sauviac, F. Mariotte, and T. G. Kharina, "Antenna model for conductive omega particles," *J. Electromagn. Waves Appl.*, vol. 11, no. 11, pp. 1509–1530, Jan. 1997.
[49] V. S. Asadchy, I. A. Faniayeu, Y. Ra'di, and S. A. Tretyakov, "Determining polarizability tensors for an arbitrary small electromagnetic scatterer," *Photon. Nanostruct. Fundam. Appl.*, vol. 12, no. 4, pp. 298–304, Aug. 2014.
[50] X.-X. Liu, Y. Zhao, and A. Alu, "Polarizability tensor retrieval for subwavelength particles of arbitrary shape," *IEEE Trans. Antennas Propag.*, vol. 64, no. 6, pp. 2301–2310, Jun. 2016.
[51] R. Alaee, M. Albooyeh, M. Yazdi, N. Komjani, C. Simovski, F. Lederer, and C. Rockstuhl, "Magnetoelectric coupling in nonidentical plasmonic nanoparticles: Theory and applications," *Phys. Rev. B, Condens. Matter*, vol. 91, no. 11, Mar. 2015, Art. no. 115119.
[52] I. Faniayeu and V. Mizeikis, "Vertical split-ring resonator perfect absorber metamaterial for IR frequencies realized via femtosecond direct laser writing," *Appl. Phys. Exp.*, vol. 10, no. 6, Jun. 2017, Art. no. 062001.
[53] R. Alaee, M. Albooyeh, A. Rahimzadegan, M. S. Mirmoosa, Y. S. Kivshar, and C. Rockstuhl, "All-dielectric reciprocal bianisotropic nanoparticles," *Phys. Rev. B, Condens. Matter*, vol. 92, no. 24, Dec. 2015, Art. no. 245130.
[54] V. Asadchy, M. Albooyeh, and S. Tretyakov, "Optical metamirror: All-dielectric frequency-selective mirror with fully controllable reflection phase," *J. Opt. Soc. Amer. B, Opt. Phys.*, vol. 33, no. 2, p. A16, 2016.
[55] V. S. Asadchy, A. Díaz-Rubio, and S. A. Tretyakov, "Bianisotropic metasurfaces: Physics and applications," *Nanophotonics*, vol. 7, no. 6, pp. 1069–1094, Jun. 2018.

HEMN YOUNESIRAAD received the B.Sc. and M.Sc. degrees in electrical engineering from the University of Tabriz, Tabriz, Iran, in 2009 and 2011, respectively, where he is currently pursuing the Ph.D. degree. He is also with the University of Tabriz. His research interests include metamaterials, metasurfaces, mantle cloaking, wireless power transfer, and electromagnetic theory.

MOHAMMAD BEMANI received the B.S. degree in electrical engineering from the K. N. Toosi University of Technology, Tehran, Iran, in 2007, and the M.S. and Ph.D. degrees from the University of Tabriz, Tabriz, Iran, in 2009 and 2014, respectively. He is currently an Assistant Professor with the Department of Electrical and Computer Engineering, University of Tabriz. His research interests include multiband and UWB components, reconfigurable antenna, dielectric resonator antennas, composite right and left-handed structures, negative-refractive index, active circuits, and antenna arrays.

LADISLAU MATEKOVITS (Senior Member, IEEE) received the degree in electronic engineering from the Institutul Politehnic din Bucureşti, Bucureşti, Romania, in 1992, and the Ph.D. degree (Dottorato di Ricerca) in electronic engineering from the Politecnico di Torino, Torino, Italy, in 1995.

Since 1995, he has been with the Department of Electronics and Telecommunications, Politecnico di Torino, as a Postdoctoral Fellowship and a Research Assistant. He joined the Department of Electronics and Telecommunications, as an Assistant Professor, in 2002, a Senior Assistant Professor, in 2005, and an Associate Professor, in 2014. In 2005, he was a Visiting Scientist with the Antennas and Scattering Department, Fraunhofer Institute (FGAN-FHR), Wachtberg, Germany. In July 2009, he was a Marie Curie Fellow with Macquarie University, Sydney, NSW, Australia, for a period of two years, where he also held a Visiting Academic position, in 2013, and an Honorary Fellow, in 2014. In February 2017, he was a Full Professor (national qualification), Italy. Since 2020, he has been an Honorary Professor with the Polytechnic University of Timisoara. He was an Assistant Chairman and the Publication Chairman with the European Microwave Week, Milan, Italy, in 2002. He also held an associate position with the Italian National Research Council. Material parameter retrieval of these structures by inverse methods and different optimization techniques has been considered. Bio-electromagnetic aspect has also been contemplated, such as design of implantable antennas or development of nano-antennas, for example, drug delivery applications. He has published over 350 articles, including more than 85 journal contributions and delivered seminars on these topics all around the world, such as Europe, USA (AFRL/MIT-Boston), Australia, China, and Russia. He was invited to serve as a Research Grant Assessor for government funding calls in Romania, Italy, and Croatia. He was also an International Expert for the Ph.D. thesis evaluation with several universities in Australia, India, Pakistan, Spain, and so on. His main research interests include numerical analysis of printed antennas and particular development of new, numerically efficient full-wave techniques to analyze large-arrays, optimization techniques, and active and passive metamaterials for cloaking applications.

Prof. Matekovits was a member of the National Council for the Attestation of University Degrees, Diplomas, and Certificates (CNATDCU), Romania. Since 2010, he has been a member of the Organizing Committee, International Conference on Electromagnetics in Advanced Applications (ICEAA). He is also a member of the technical program committees of several conferences. He served as the General Chair for the 11th International Conference on Body Area Networks (BodyNets), in 2016. He was a recipient of various awards in international conferences, including the 1998 URSI Young Scientist Award, Thessaloniki, Greece, the Barzilai Award in 1998 (Young Scientist Award, granted every two years from the Italian National Electromagnetic Group), and the Best AP2000 Oral Paper on Antennas, ESA-EUREL Millennium Conference on Antennas and Propagation, Davos, Switzerland. He was also a recipient of the Motohisa Kanda Award for the most cited paper from the IEEE TRANSACTIONS ON ELECTROMAGNETIC COMPATIBILITY in the past five years, in 2018. He received the 2019 American Romanian Academy of Arts and Sciences (ARA) Medal of Excellence in Science. He serves as an Associate Editor for IEEE ACCESS, the IEEE ANTENNAS AND WIRELESS PROPAGATION LETTERS, and *IET MAP*. He also serves as a Reviewer for different journals.